Acta Biomaterialia 116 (2020) 246–258

Contents lists available at ScienceDirect

Acta Biomaterialia

journal homepage: www.elsevier.com/locate/actbio

Full Length Article

Riboflavin-mediated photooxidation to improve the characteristics of decellularized human arterial small diameter vascular grafts

Karl H. Schneider[a,b], Sabrina Rohringer[a,b], Barbara Kapeller[a], Christian Grasl[b,c], Herbert Kiss[d], Stefan Heber[e], Ingrid Walter[f], Andreas H. Teuschl[g,h], Bruno K. Podesser[a,b,i], Helga Bergmeister[a,b,i,*]

[a] Medical University of Vienna, Center for Biomedical Research, Austria
[b] Ludwig Boltzmann Institute for Cardiovascular Research, Vienna, Austria
[c] Medical University of Vienna, Austria
[d] Medical University of Vienna, Center for Medical Physics and Biomedical Engineering, Department of Obstetrics and Gynecology, Division of Obstetrics and Feto-Maternal Medicine, Austria
[e] Medical University of Vienna, Center for Physiology and Pharmacology, Institute of Physiology, Vienna, Austria
[f] University of Veterinary Medicine Vienna, Department of Pathobiology, Austria
[g] University of Applied Sciences Technikum Wien, Vienna, Austria
[h] Department of Biochemical Engineering, City of Vienna Competence Team Signal Transduction, Vienna, Austria
[i] Austrian Cluster for Tissue Regeneration, Vienna, Austria

ARTICLE INFO

Article history:
Received 11 May 2020
Revised 27 July 2020
Accepted 25 August 2020
Available online 29 August 2020

Keywords:
Small diameter vascular graft
Human placenta
Decellularization
Surface modification
Biomechanical strength
Dye mediated photooxidation

ABSTRACT

Vascular grafts with a diameter of less than 6 mm are made from a variety of materials and techniques to provide alternatives to autologous vascular grafts. Decellularized materials have been proposed as a possible approach to create extracellular matrix (ECM) vascular prostheses as they are naturally derived and inherently support various cell functions. However, these desirable graft characteristics may be limited by alterations of the ECM during the decellularization process leading to decreased biomechanical properties and hemocompatibility. In this study, arteries from the human placenta chorion were decellularized using two distinct detergents (Triton X-100 or SDS), which differently affect ECM ultrastructure. To overcome biomechanical strength loss and collagen fiber exposure after decellularization, riboflavin-mediated UV (RUV) crosslinking was used to uniformly crosslink the collagenous ECM of the grafts. Graft characteristics and biocompatibility with and without RUV crosslinking were studied *in vitro* and *in vivo*. RUV-crosslinked ECM grafts showed significantly improved mechanical strength and smoothening of the luminal graft surfaces. Cell seeding using human endothelial cells revealed no cytotoxic effects of the RUV treatment. Short-term aortic implants in rats showed cell migration and differentiation of host cells. Functional graft remodeling was evident in all grafts. Thus, RUV crosslinking is a preferable tool to improve graft characteristics of decellularized matrix conduits.

Statement of significance

The design of a successful small-diameter vascular graft with desirable characteristics is still a challenge. Currently, there are no sufficient alternatives to autologous grafts available. Decellularized matrix grafts seem to be promising candidates to overcome these limitations. However, properties of naturally derived materials may be changed by the decellularization process, resulting in reduced biomechanical properties and hemocompatibility. Therefore, we show in this study that riboflavin-mediated crosslinking is an effective approach to improve biomechanical strength and surface topography of human placenta-derived matrix grafts after decellularization.

1. Introduction

Autologous vessels such as saphenous vein, internal mammary artery and radial artery are currently the materials of choice for

* Corresponding author.
E-mail address: helga.bergmeister@meduniwien.ac.at (H. Bergmeister).

https://doi.org/10.1016/j.actbio.2020.08.037
1742-7061/

vascular transplants with small diameters (<6 mm), because of high patency rates [1]. However, using the patient's own tissue requires invasive harvesting procedures and availability might be limited due to pre-existing disease or repetitive surgery.

Several types of vascular grafts have been developed to overcome current limitations of small diameter vascular replacement. [2–6]. Synthetic vascular prostheses materials can be fabricated with high reproducibility and can be easily modified. Synthetic substitutes have demonstrated high long-term patency rates when applied in large diameter arteries (>6 mm). However, when used as small diameter (<6 mm) vascular grafts, they show unacceptably low patency rates [7,8]. For that reason, biological vascular grafts derived from the extracellular matrix (ECM) of arteries gained importance as alternative material [9–13].

Decellularized human arteries from the placenta chorion have shown potential as small diameter vascular grafts because of their low immunogenicity as well as optimal support for both cell migration and growth after implantation [14]. However, the decellularization process alters the structure of the vascular graft matrix [15–20]. Successful decellularization is always a compromise between the complete removal of cells and their cell residues (e.g. DNA) and the structural degradation of ECM proteins such as collagen or proteoglycans.

Various decellularization approaches have been investigated with the aim to overcome these limitations. Besides biological and chemical approaches, physical decellularization methods such as freeze/thaw cycles, mechanical agitation, sonication or exposure to supercritical CO2 have been proposed to preserve the ultrastructure of the tissue particularly well [21,22]. However, none of these protocols alone meets all the desired requirements for tissue decellularization, and often a combination of different protocols is required to meet the criteria for effective decellularization [23]. Subsequent to this process, clinical application is only conceivable through intensive evaluation of the biological properties of the tissue produced [24].

In this study, we used a previously described detergent based pulsatile flow decellularization technique for vascular grafts which enables the use of lower chemical concentrations and exposure times. It has been shown that this procedure removes cells sufficiently and improves the preservation of the ECM [25]. However, our previous studies have shown that even with this set-up the biomechanical strength of ECM grafts was reduced in comparison to native blood vessels. Beside degradation of structural proteins, the luminal cell layer is completely removed in the arterial ECM graft during decellularization and collagen fibers are exposed to the lumen of the vessels [18]. This may cause blood clotting after implantation. It has been shown previously that hemocompatibility of ECM grafts can be improved by covalently bound heparin molecules to the collagenous surface [9,14].

The here presented study counteracts the loss of mechanical strength and collagen exposure at the luminal surface of the conduits after decellularization. Collagen fibers of ECM grafts can be crosslinked by chemical or physical treatment. Chemically, aldehydes, isocyanates or carbodiimides are used as crosslinking agents. Physically crosslinking methods are UV irradiation or dehydrothermal methods. Both techniques have in common to mediate new covalent bonds at the amine and carboxyl groups within the collagen molecules [26,27]. However, chemical crosslinking agents such as glutaraldehyde may be effective, but are cytotoxic when not completely removed and often lead to graft failure, calcification and inhibited cell migration after implantation [12]. UV light treatment alone often leads to denaturation of the scaffold and is only suitable for grafts showing thin walls since the light wave cannot pass thick tissues [28]. We wanted to overcome these limitations by using a photosensitizer in combination with UV irradiation, as it has been used previously to improve the biomechanical properties of collagen scaffolds [29]. In various studies dye-Mediated Photo-Oxidation has been shown to be a promising alternative to chemical crosslinking to generate biostable implants being resistant to calcification and showing low immunogenic response [30,31]. Here, we evaluated the effectiveness of riboflavin mediated UV (RUV) crosslinking to improve the mechanical characteristics and hemocompatibility of decellularized arteries from placental chorion. Two detergent based protocols which are reported to have different effects on ECM structure and components were applied to investigate the effect subsequent of RUV crosslinking. A harsh, ionic detergent for decellularization (SDS), which is known to be efficient in removing nuclei but rather destroys the ECM, and a non-ionic and comparable mild detergent (Triton), which preserves GAG and growth factors better, were included in this study. Besides characterization of surface topography, platelet adhesion, cell viability, and biomechanical strength *in vitro*, short term implantation studies in rats were performed to assess graft performance, cell migration and functional remodeling *in vivo*.

2. Materials and Methods

2.1. Human placenta harvesting

Human placenta tissues were obtained from the Department of Obstetrics and Gynecology, Medical University of Vienna, with approval from the institutional ethics committee (EK:1602/2018) and informed consent from all donors. Placentas were harvested after planned caesarian section deliveries at term (pregnancy week 37 + 0 to 40 + 0). The placental vascular tree was rinsed with phosphate buffered saline (PBS) supplemented with heparin (50 IU/ml) and antibiotics (1% penicillin/streptomycin). The vessels were freed from remaining blood and the whole placenta was frozen at -80°C until decellularization. Thereafter the placenta vessels were further processed as indicated in our flow scheme (Fig. 1). All donors were serologically tested for HIV, HBV and HCV.

2.2. Decellularization

Blood vessels were decellularized using either Triton-X 100 or Sodium Dodecyl Sulfate (SDS) and enzymatic digestion as previously described [14]. Briefly, after isolation from the chorionic plate, vessels underwent a freeze-thaw cycle at -80°C for 18 h. Afterwards, they were washed with PBS and subjected to a perfusion system using a peristaltic pump at pressure levels ranging from 60–80 mmHg (Minipuls Evolution, Gilson, USA). Vessels were perfused with hypertonic (1.2% NaCl) and hypotonic (0.4% NaCl) saline solutions for 30 min each followed by perfusion with PBS containing 1% Triton X-100 (Sigma-Aldrich, Austria) or 0.5% SDS and 0.02% ethylene-diaminetetraacetic acid (EDTA) for 24 h at room temperature. Subsequently, vessels were thoroughly washed with PBS for 18 h before an overnight incubation at 4°C with DNAse I-solution (200 IU/ml, Roche, Switzerland) was performed. Chemical sterilization was carried out by rinsing the vessels with sterile PBS followed by a washing step with 0.18% (w/v) peracetic acid (PAA) and 4.8% EtOH solution at pH 7.0 [32]. Samples from each batch were routinely evaluated for a successful decellularization process by using histological staining in conjunction with biochemical quantification of DNA, collagen and proteoglycans.

2.3. Riboflavin-mediated UV (RUV) crosslinking

Riboflavin (Vitamin B2) powder was diluted to 0.1% in a 20% Dextran T500 aqueous solution. Vessels were incubated within the photosensitizer solution in a petri dish under UVC light (253 nm) in a laminar flow hood for 60 min. After RUV crosslinking, vessels were rinsed with distilled water three times. The vessels were subjected to 50 ml conical falcon tubes and washed three times with

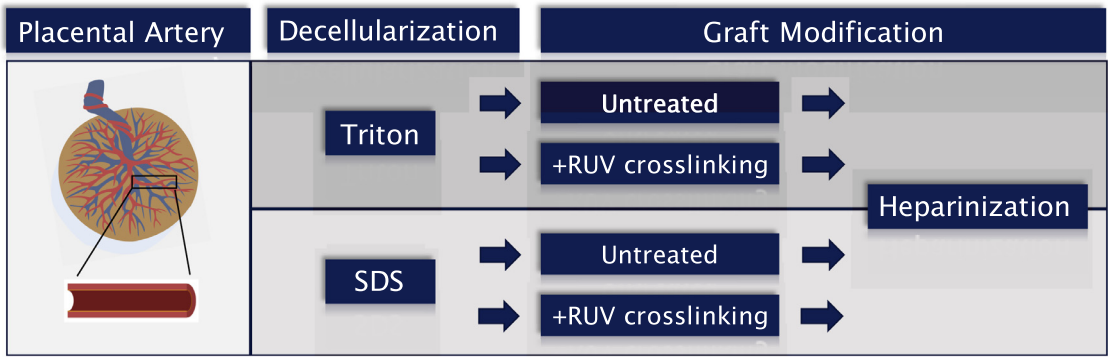

Fig. 1. Experimental setup. After decellularization with either Triton or SDS, grafts were left untreated or were RUV crosslinked. Finally, the luminal surface of all grafts was modified by heparin crosslinking.

PBS for 20 min and afterwards stored at 4°C in PBS before further use.

2.4. Heparinization

For heparinization of the grafts, vessels were incubated in 1 M hydroxylamine sulfate aqueous solution for 18 h in 50 ml falcon tubes on a roller shaker. On the next day, the hydroxylamine sulfate solution was aspirated and vessels were washed twice with distilled water for 30 min after transfer in new falcon tubes. During the water change after 30 min, the vessels were additionally rinsed with distilled water in a petri dish once. Subsequently, vessels were perfused with heparin solution (500 U/ml heparin + 1.25% N'-ethylcarbodiimide hydrochloride (EDC), adjusted to pH 1.5 with HCl, sterile filtered) for 48 h on a roller shaker at room temperature. After the incubation time, vessels were washed with distilled water for 1.5 h and further with PBS at room temperature for 2.5 h. Vessels were then stored in PBS overnight. After 24 h the specimens were rinsed with sterile PBS in a laminar flow hood.

2.5. Biomechanical testing

Biomechanical properties of the grafts were evaluated by ultimate tensile tests and suture retention tear-out tests. Ultimate tensile testing was performed using an uniaxial BOSE Electroforce LM1 test bench system (Bose Corp, USA) as described previously [33]. Briefly, ring segments of 3 mm length were cut from the chorionic vessels (n = 12), put on 0.6 mm steel hooks and strained till failure (10 mm/min) in a 37°C saline bath before and after RUV treatment as well as prior and after 1 month of implantation. Specimens of all groups were tested for maximal tensile force and compliance. The compliance (% diameter change/100 mmHg) and the theoretical burst pressure were determined using Laplace's law [33].

The suture retention strength was determined according to the test method described in ISO 7198:2016 [34]. Briefly, one end of the grafts was clamped to the tensile testing machine (Messphysik Beta 10-2,5, Messphysik Materials Testing GmbH, Austria). As shown in Fig. 4E, a loop of a 7.0 polypropylene suture (Prolene, BV 176-8, USA) was sutured 2 mm from the edge of the free end of the sample into the graft wall and clamped to one arm of the tensile tester. The opposite end of the sample was directly clamped to the other arm of the testing machine. The tear-out force of the suture was measured at a loading speed of 120 mm/min. Five tests per sample were carried out (n = 6). Native placental arteries served as controls in all biomechanical experiments.

2.6. Contact angle and wettability

Contact angles of decellularized matrices were evaluated to determine surface wettability and to detect possible alterations upon RUV treatment and/or heparinization. Therefore, captive air-bubble contact angles were measured by the inverted drop method using a goniometer (Data Physics, model OCA 15, Germany) equipped with a video CCD-camera. Accordingly, each sample was longitudinally opened attached to a microscope slide and placed into an ultrapure water-filled glass chamber. After that, a 10 μL air bubble was released from a J-shaped needle underneath the sample's surface and the contact angle was measured at the luminal surface using the software SCA (Kiuwan, USA).

2.7. Cell Culture

If not otherwise stated, all cell culture materials including cells and supplements were purchased from Thermo Fisher Scientific (Waltham, USA). Human umbilical vein endothelial cells (HUVEC) from passage 2 to 8 were cultured in Medium 200 supplemented with low serum growth supplement, 8% fetal calf serum (FCS) and 1% penicillin/streptomycin. Sub-culturing of cells was performed at 80% confluence in a splitting ratio of 1:3 or 1:4 by trypsinization. Human foreskin fibroblasts (HFF, ATCC, USA) were cultured in high glucose Dulbecco's Modified Eagle Medium supplemented with 10% FCS, 1% non-essential amino acids and 1% penicillin/streptomycin.

2.8. Cell viability assay

Decellularized vessel grafts were cut into 2 × 2 mm pieces and transferred into a 96 well plate. Graft pieces were washed with PBS twice. 1 × 10^4 HUVEC (p2-p8) were seeded per graft on day 0. HUVECs were seeded on the luminal side of the graft pieces. After cell attachment and immediately before XTT solution was added to the wells graft pieces were transferred to a new 96 well plate to ensure that the viability is only evaluated from cells seeded on the graft. The pieces were humidified with 200 µl cell culture medium. XTT assay was performed on days 3, 6 and 8 after seeding. For the measurement, the wells were complemented with 50 µl XTT working solution (25 µM phenazine methosulfate with 1 mg/ml 3,3'-(1-[(phenylamino)carbonyl]-3,4-tetrazolium)-bis(4-methoxy-6-nitro) benzene sulfonic acid hydrate (both Sigma-Aldrich). The plates were incubated for 4 h at 37°C. Thereafter, the supernatant was transferred to a new 96 well plate to avoid background signal from the graft piece and absorption was measured at 450–490 nm (reference wavelength 620–650 nm) with a Powerwave XS2 microplate reader (Biotek, USA). The effects of detergent (SDS and Triton), RUV (without and with) and time

(3d, 6d, 8d) on HUVEC proliferation were tested by a 3-factorial ANOVA.

2.9. Platelet adhesion

Platelet enrichment was performed as described before [35]. Briefly, 45 ml of citrated whole blood were obtained from healthy donors and diluted with PBS in a 1:1 ratio. The blood was pipetted onto a layer of Ficoll Paque (GE Healthcare, USA) and density centrifugation was performed for 30 min at 300 g without brake. The upper phase and buffy coat were transferred into a new tube and centrifuged again at 300 g for 10 min. The upper 2/3 of the solution was aspirated (platelet poor plasma) and the remaining cells and fluid were resuspended (platelet rich plasma (PRP). Cells were counted and diluted to a concentration of 20×10^6 cells/ml. Graft pieces were subjected to a 24 well plate and seeded with PRP for 2 h on the luminal surface with gentle shaking every 10 min. Cells were then fixed in 2.5% glutaraldehyde for 2 hours at 4°C before the samples were dried and prepared for scanning electron microscopy. Furthermore, dehydrated samples were stained with 10 mM mepacrine solution (Sigma-Aldrich, USA) for 90 min at room temperature, followed by three washing steps with PBS. Images were taken on a Zeiss LSM 700 confocal microscope (Zeiss, Germany).

2.10. Scanning electron microscopy

Graft samples were fixed in 2.5% glutaraldehyde (in PBS) for 18 h and subjected to ethanol series ranging from ethanol concentrations of 25% up to 100%. Thereafter, hexamethyldisilazane (HMDS) was pipetted on top of the samples and the samples were dried overnight under a fume hood. Chemically dried samples were sputter coated with 20 nm of gold and analyzed with a Zeiss EVO 10 (Zeiss, Austra).

2.11. Immunofluorescence staining

HUVECs were seeded to the luminal side of either non-treated or RUV-treated graft pieces for one week. To evaluate the formation of a consistent monolayer, cells were then fixed with 4% buffered formaledehyde overnight at 4°C. Samples were stained with a fluorescein isothyocyanate (FITC) labeled anti-CD31 antibody (BD Biosciences, USA) by an overnight incubation in PBS supplemented with 1% bovine serum albumin (BSA, Sigma-Aldrich, USA) in a dilution of 1:50. After three washing steps with PBS, samples were subjected to microscopy slides with fluorescent mounting medium (Dako, USA) including 1 µM 4',6-Diamidin-2-phenylindol (DAPI, Sigma-Aldrich, USA). Imaging was performed at a Zeiss LSM 700 confocal microscope (Zeiss, Germany).

2.12. Histology

Grafts were fixed in 4% buffered formaldehyde for 48 h. Tissues were then dehydrated by an ascending series of ethanol and embedded in paraffin through xylene as intermedium, using an automated embedding device (TissueTek VIP 6, Sakura Finetek USA, Inc., Torrance, CA, USA). Sections of 3 µm thickness were cut and stained with hematoxylin and eosin (H&E) according to Romeis [36] for general morphological evaluation. Immunofluorescence staining was performed to investigate cell migration, proliferation and tissue remodeling. To determine the cell number within the grafts and the proliferation activity of immigrated cells a ki67 staining was performed and both ki67-positive nuclei and ki67-negative nuclei, counter-stained with DAPI, were counted with image analyzing software FIJI as described before [37]. A 3-way ANOVA was used to statistically evaluate a possible effect of RUV on cell proliferation *in vivo*. The exact protocol, including all used materials are described in the Supplemental method section in detail. A triple-immunofluorescence staining, using antibodies against calponin, smooth muscle actin and vimentin, was performed to evaluate tissue remodeling.

2.13. Animal model

The animal studies were approved by the Austrian Ministry of Science. All animals received humane care within the principles of the Good Scientific Practice (GCP) Guidelines of the Medical University of Vienna. Procedures were performed under general anesthesia as previously described [9].

Heparinized grafts of both groups (Triton/SDS) with and without RUV crosslinking were implanted aseptically into the infrarenal aorta of Sprague Dawley rats as earlier described [5]. The grafts (inner diameter: 2 mm, length: 20 mm) were inserted into the host vessel using a surgical microscope (Zeiss Vario S88, Carl Zeiss GmbH, Vienna, Austria). The end-to-end anastomoses were performed with 10/0 non-absorbable sutures (Monosoft, Covidien, Mansfield, USA).

No anticoagulants or anti-platelet drugs were administered during and after the *in vivo* study. Retrieved grafts were subjected to different analyses. After 1 month, the midgraft region was cut into three pieces and analyzed by scanning electron microscopy (SEM), histology and biomechanical testing. Further proximal and distal anastomoses were evaluated by histology.

2.13. Electromyography

Isometric tension studies were performed as described previously [14]. Briefly, at retrieval, ring shaped specimens of 2 mm length from each group were cut from the mid-graft region, laced in 4°C cold Krebs Buffer solution and immediately measured. Native rat aorta segments were used as controls. For measurement of the contractile force a 620 M Multi Wire Myograph System (ADInstruments, Oxford, UK) was used. Therefore, the segments were mounted on two metal pins in a myograph chamber filled with preheated (37°C) and aerated (95% O_2, 5% CO_2) Krebs-Buffer solution. Each ring was stretched to a baseline tension of 10 mN for normalization and equilibrated for 45 min. At increased potassium levels (60 mM K^+) in the chamber natural contraction of the blood vessel segments was induced. The datapoints of contractile force were recorded and processed using LabChart Pro V8 software (ADInstruments, UK).

2.14. Statistical methods

The primary research question, whether RUV crosslinking improves mechanical strength of decellularized placental arteries, was tested using mixed linear models. After testing interactions, the effect of RUV was plotted as a single estimate applying for all conditions with its 95% confidence interval. All analyses were performed using IBM SPSS Statistics 26 (IBM, USA), graphs were generated using GraphPad Prism 8 (GraphPad, USA). All reported p-values are the results of two-sided tests. P-values ≤ 0.05 were considered to be statistically significant. Due to the exploratory, basic science character of this study no adjustment for multiple testing was performed. Results have to be interpreted accordingly. Detailed statistical analyses are described in the supplement methods section.

3. Results

3.1. Efficacy of blood vessel decellularization

Histological staining showed no signs of cell nuclei after decellularization. The DNA content was significantly reduced in both de-

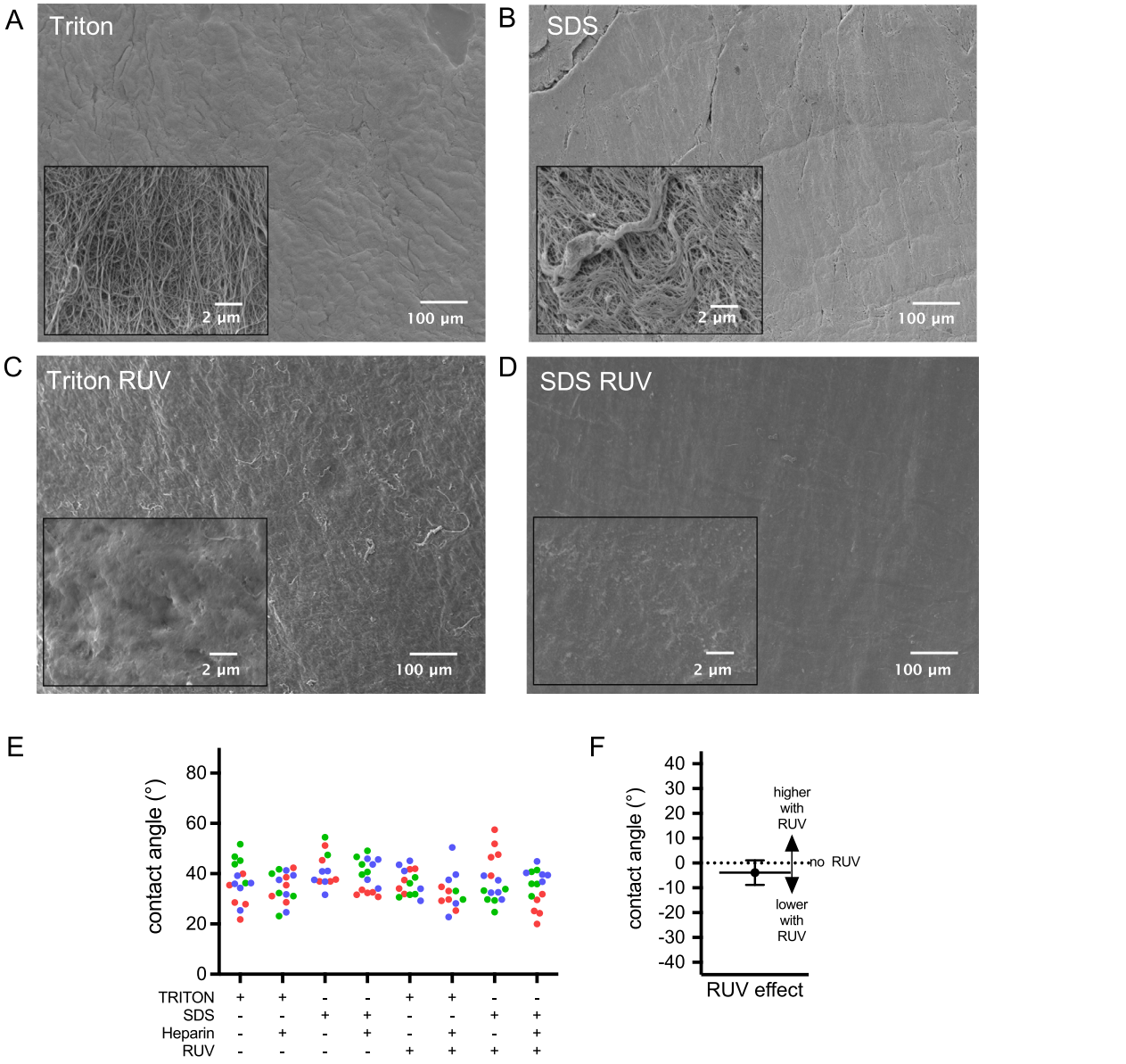

Fig. 2. (A–D) Surface topography of luminal graft surfaces prior and after RUV crosslinking. A strong smoothening effect of RUV treatment in both decellularization groups sodium dodecyl sulfate (SDS) and Triton X-100 (Triton) is evident. (E) Air bubble contact angle measurement of decellularized ECM grafts at different stages of surface modification. Contact angles between 30 and 40 degrees indicate rather hydrophilic surfaces. (F) Estimated main effect of RUV on contact angles with 95% confidence interval including 0, indicating that RUV application did not significantly affect wettability.

cellularized conduits by over >97%, whereas collagenous structures could be preserved in both protocols. The content of proteoglycans (GAG) was significantly reduced in both decellularization groups. SDS treated grafts showed significantly less preserved GAG (Suppl. Fig. 1).

3.2. Matrix graft topography and wettability

According to scanning electron microscopy, RUV treatment of decellularized vessels appeared to smoothen the initially rough surface (Fig. 2A-D). The captive air-bubble contact measurements, designed to quantify wettability, showed that neither the type of detergent ($p = 0.62$), heparinization ($p = 0.38$), or RUV treatment ($p = 0.12$) significantly affected contact angles (all interaction terms $p > 0.15$, Fig. 2E & F; Suppl. Fig. 2). The grand mean of contact angles was 36.8° (95% CI 34.3–39.3), indicating that mean contact angles were significantly lower than 39.3°. As a contact angle below 90° indicates hydrophilic surface structures, the graft material itself showed high hydrophilicity, i.e. wettability [38].

3.3. High cell viability and reduced platelet adhesion on RUV crosslinked grafts

The investigation of HUVEC adhesion, proliferation, and viability showed that cells maintain their morphology and proliferate on RUV crosslinked vessel pieces *in vitro* (Fig. 3A & B). The effects of detergents (SDS and Triton), RUV (without and with) and time (3d, 6d, 8d) on HUVEC proliferation were tested by an XTT assay (Fig. 3C). While HUVEC proliferation significantly increased during the observational period (main effect of time $p < 0.0001$), there was neither an effect of the detergent (main effect of detergent and all interaction terms containing detergent $p > 0.26$) nor of RUV (main effect of RUV and all interaction terms containing RUV $p > 0.26$).

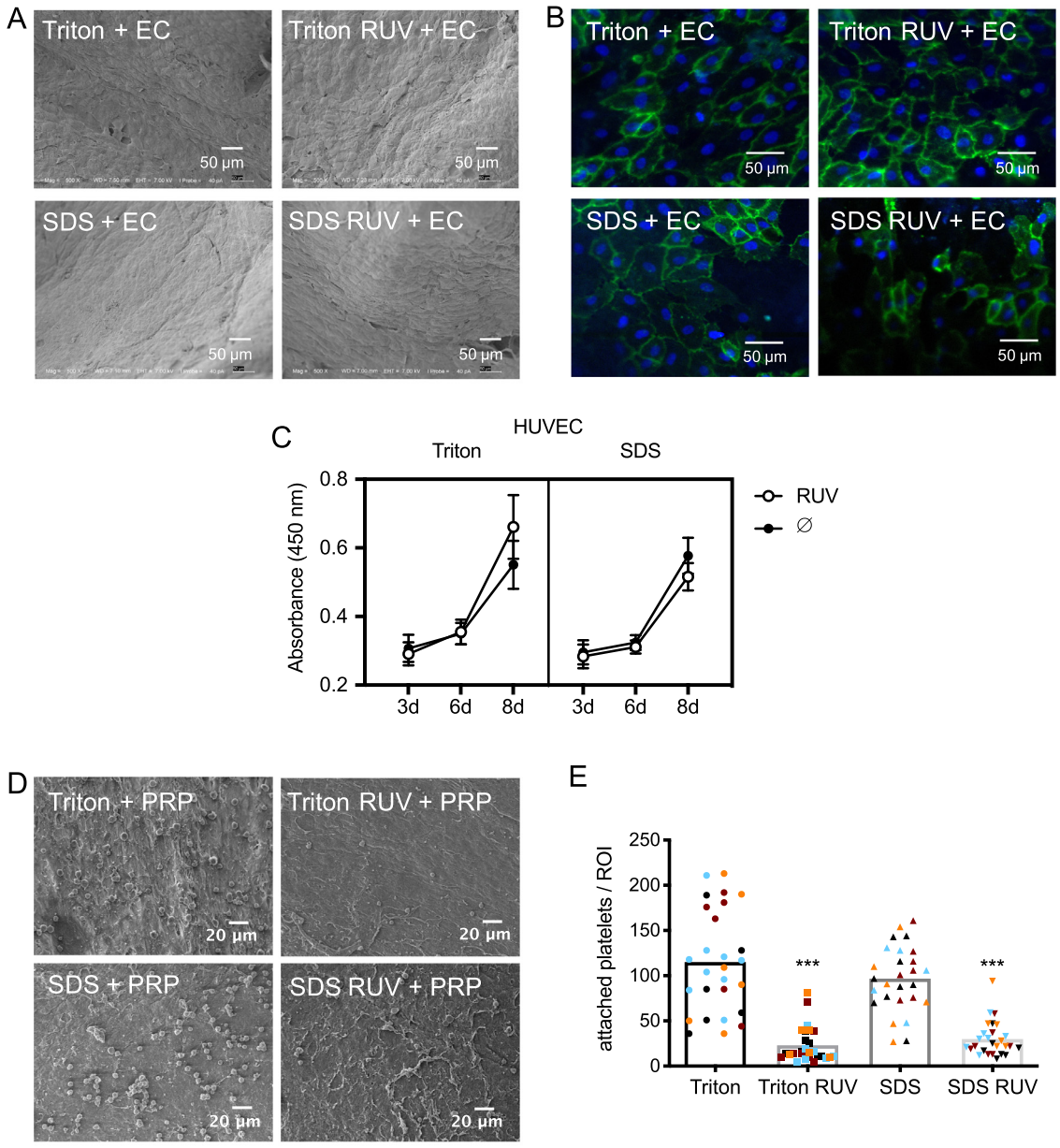

Fig. 3. Luminal graft surface after reseeding with human umbilical vein endothelial cells (HUVEC). (A) Scanning electron microscopy, (B) confocal electron microscopy (immunofluorescence staining, CD31 – green, DAPI – blue). (C) RUV treatment revealed no change of proliferation rates in HUVEC analyzed by XTT proliferation assay (n = 3). (D) Significantly decreased platelet adhesion on RUV-treated placental ECM grafts was observed after 2 h incubation with platelet rich plasma (PRP) solution. (E) Effect of decellularization and RUV treatment on platelet attachment. Each color within a group represents a graft (4 grafts / group), each symbol represents platelet counts in a certain graft area (platelets in 7 graft areas were quantified).

To test if RUV crosslinking would be beneficial for reduced platelet adhesion to grafts, platelets were isolated from whole blood and seeded on graft pieces for two hours. RUV crosslinking decreased platelet adhesion by 77% (95% CI 70–83%, $p < 0.0001$) (Fig. 3D & 3E and Suppl. Fig. 4). The effect was similar in Triton- and SDS-treated grafts ($p = 0.06$).

3.4. Increased biomechanical strength and suture retention

Fig. 4A demonstrates the setup for mechanical testing. Segments of graft specimens showed a significantly increased maximal radial force of 0.83 N due to RUV treatment (95% CI 0.46–1.2, $p < 0.0001$, Fig. 4B). Although the effect of RUV appeared to be smaller post-implant compared to pre-implant, there was no evidence that the effect of RUV was affected by vessel implantation or type of detergent (3-way interaction and all three 2-way interactions, $p > 0.1$ each). Furthermore, there was no evidence that the effect of RUV on burst pressure was affected by the type of detergent or by implantation (3-way interaction and two 2-way interactions including RUV, $p > 0.26$ each). Calculated burst pressure was also increased by RUV, namely by 942 mmHg (95% CI 581–1303, $p < 0.0001$, Fig. 4C).

While the readouts which were mentioned above indicate higher biomechanical strength, there was no evidence that RUV had a relevant effect on vessel compliance (difference with vs. without RUV 0.65%, 95% CI -0.5–1.9, $p = 0.24$, Fig. 4D). However,

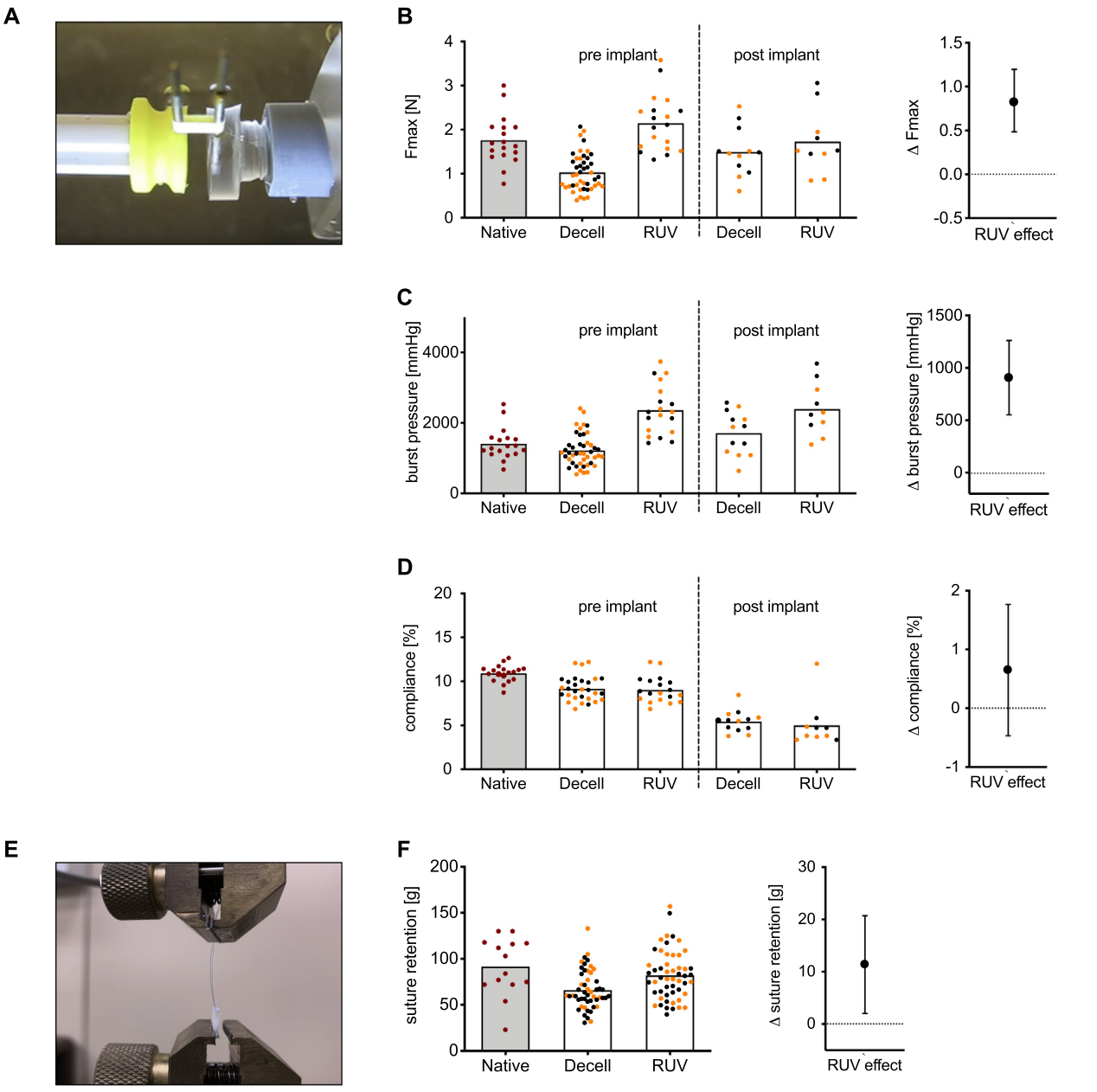

Fig. 4. Effect of RUV crosslinking on biomechanical properties of placental ECM grafts pre and post implantation (A) 3 mm graft segments on metal pins of the Bose uniaxial test system in 37°C warm physiological saline solution. RUV treatment significantly improved tensile strength (B), burst pressure (C) and suture retention strength (F) of decellularized conduits, but had no effect on compliance (D) prior implantation. Each dot represents an analyzed segment. Native indicates no decellularization (grey bars with red dots), Triton (black dots) and SDS (orange dots) indicates the respective decellularization method. The estimated effect of RUV applies to all conditions, i.e. is independent of detergent or implantation. The error bar represents the 95% confidence interval. (E) Suture retention strength was determined according to ISO 7198:2016.

implantation reduced compliance from 9.4% (decellularized pre-implant) by 3.0% (95% Ci 1.9–4.1, $p < 0.0001$) to 6.4% (decellularized, post-implant) independent of RUV treatment.

In line with the results from the uniaxial tests, suture retention strength was also increased by RUV. Fig. 4E shows the experimental setup. RUV treatment increased this pull out strength by 11.4 g (95% CI 2–20.7, $p = 0.018$, Fig. 4F), whereby again, there was no evidence that this was affected by the type of detergent (interaction detergent x RUV, $p = 0.43$).

3.5. In vivo *performance of aortic implants*

The implantation of grafts into Sprague Dawley rats for one month revealed no visible signs of thrombus formation, vasodilatation or luminal narrowing in any grafts (Suppl. Fig. 5). Successful anticoagulation by heparinization of the grafts has been confirmed *in vitro* by a whole blood incubation experiment (data not shown). After one month of implantation, all grafts were integrated into the surrounding tissue (Fig. 5A). Gross examination of the conduits demonstrated a smooth and shiny inner surface without evidence of clot formation, luminal narrowing or aneurysm formation. Scanning electron microscopic analysis of the luminal surface showed complete endothelialization of all specimens (Fig. 5B). Blood samples of the animals showed slightly increased neutrophils, but no signs of severe foreign body reaction or systemic inflammation independent on the decellularization or RUV treatment (Suppl. Fig. 7).

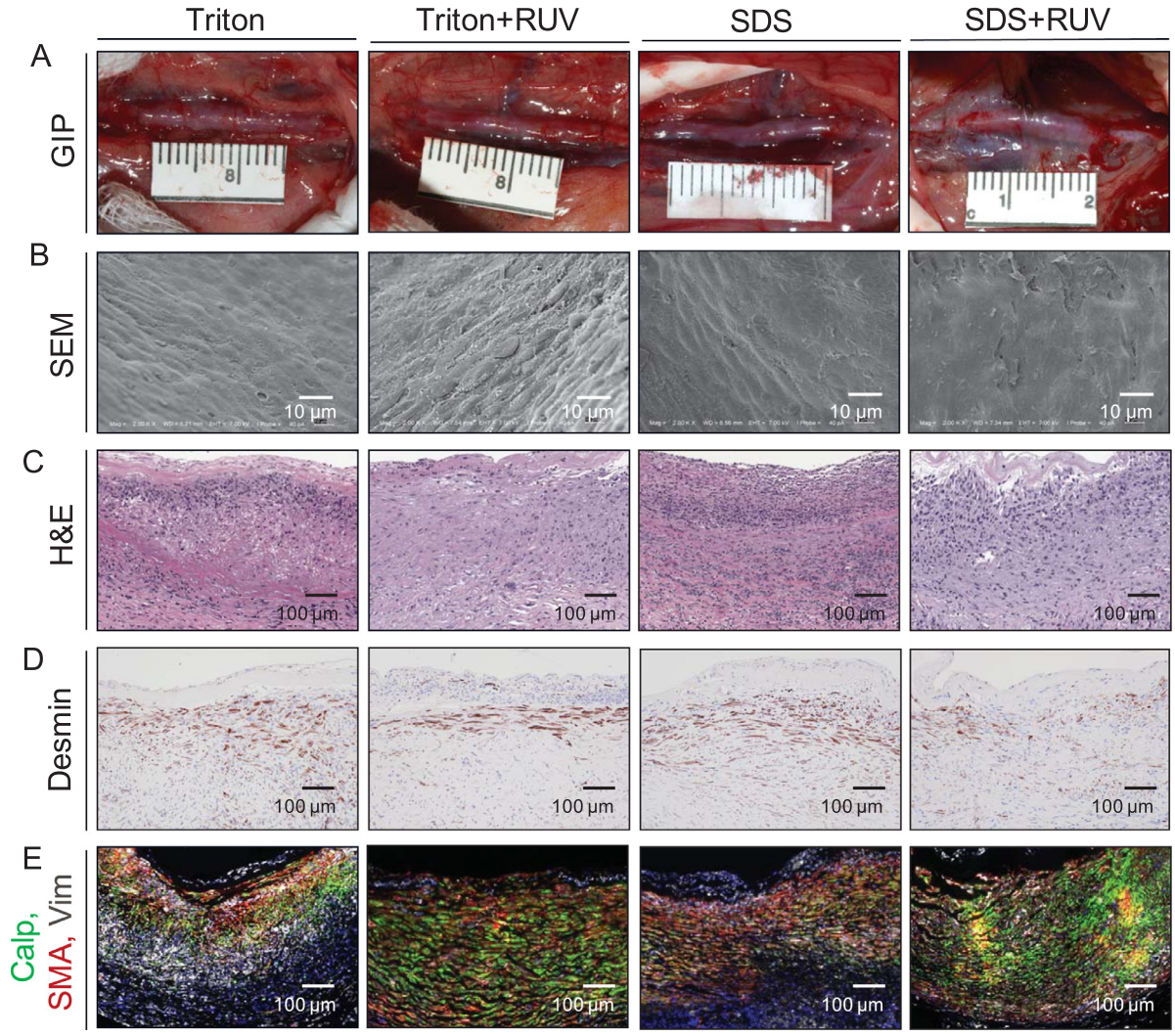

Fig. 5. (A) Gross morphology of decellularized matrix grafts implanted into the abdominal aorta of rats for1 month. (B) Scanning electron microscopic (SEM) analysis shows complete reendothelialization of the luminal surface of all specimens (scale bars: 20 µm). (C) Histological staining (H&E), (D) immunohistochemical staining for differentiated smooth muscle cells (desmin), and (E) triple immunofluorescence staining. Vimentin (Vim, grey), smooth muscle actin (SMA, red), calponin (Calp, green), nuclei (blue).

H&E staining of grafts showed that host cells had migrated from the lumen and from the adventitial side into the vessel walls within one month of implantation, both in grafts that were subject to RUV crosslinking and in those that were untreated (Fig. 5C). No signs of intimal thickening were evident. Immunohistochemical staining revealed desmin-positive smooth muscle cells in the graft wall (Fig. 5D). While there was no evidence that the type of detergent had any influence on the number of immigrated cells, a trend was observed that RUV treatment prior to implantation reduced the number of immigrated cells from 17.8×10^3 per cross-sectional area to 9.8×10^3 (main effect of RUV $p = 0.035$). Multiplex immunofluorescence (Fig. 5E) revealed the presence of a mixed population of differentiated functional smooth muscle cells (calponin+, SMA+), myofibroblasts (SMA+, vimentin+) and fibroblasts (vimentin+, SMA^-) within the graft wall. Vimentin positive cells were rather regularly distributed within the graft wall in all specimens irrespective from treatment. In RUV treated grafts we observed the presence of smooth muscle cells in all areas of the graft wall, which differed from untreated grafts, where smooth muscle cells were located only in areas close to the luminal surface (Fig. 6). In addition, myofibroblasts were present in the vascular wall of all graft types.

3.6. Recovered vasoconstriction

Functional tissue remodeling was assessed with electromyography using a DMT myograph system to measure reactive vasoconstriction in graft segments (Fig. 7A). There was no evidence that the type of detergent or RUV treatment had an effect on contractility ($p = 0.25$). Taken together, decellularized grafts showed a mean contractile force of 1.99 mN (95% CI 1.68–2.30), which is significantly greater than 0, as measured in decellularized (acellular) grafts prior implantation ($p < 0.0001$, Fig. 7B), i.e. treated grafts regained contractile capacity while being implanted. The contractile response, however, was still 2.37 mN (95% CI 1.62–3.12, $p < 0.0001$, Fig. 7C & D) lower than the response of native vessels.

4. Discussion

There is a clear need for artificial grafts with improved functional characteristics and patency rates to overcome current limitations in cardiovascular surgery and to provide an adequate alternative to autologous blood vessel grafting. Graft wall architecture, surface topography and biomechanical properties play crucial roles in graft patency. As a consequence, incompatible graft characteris-

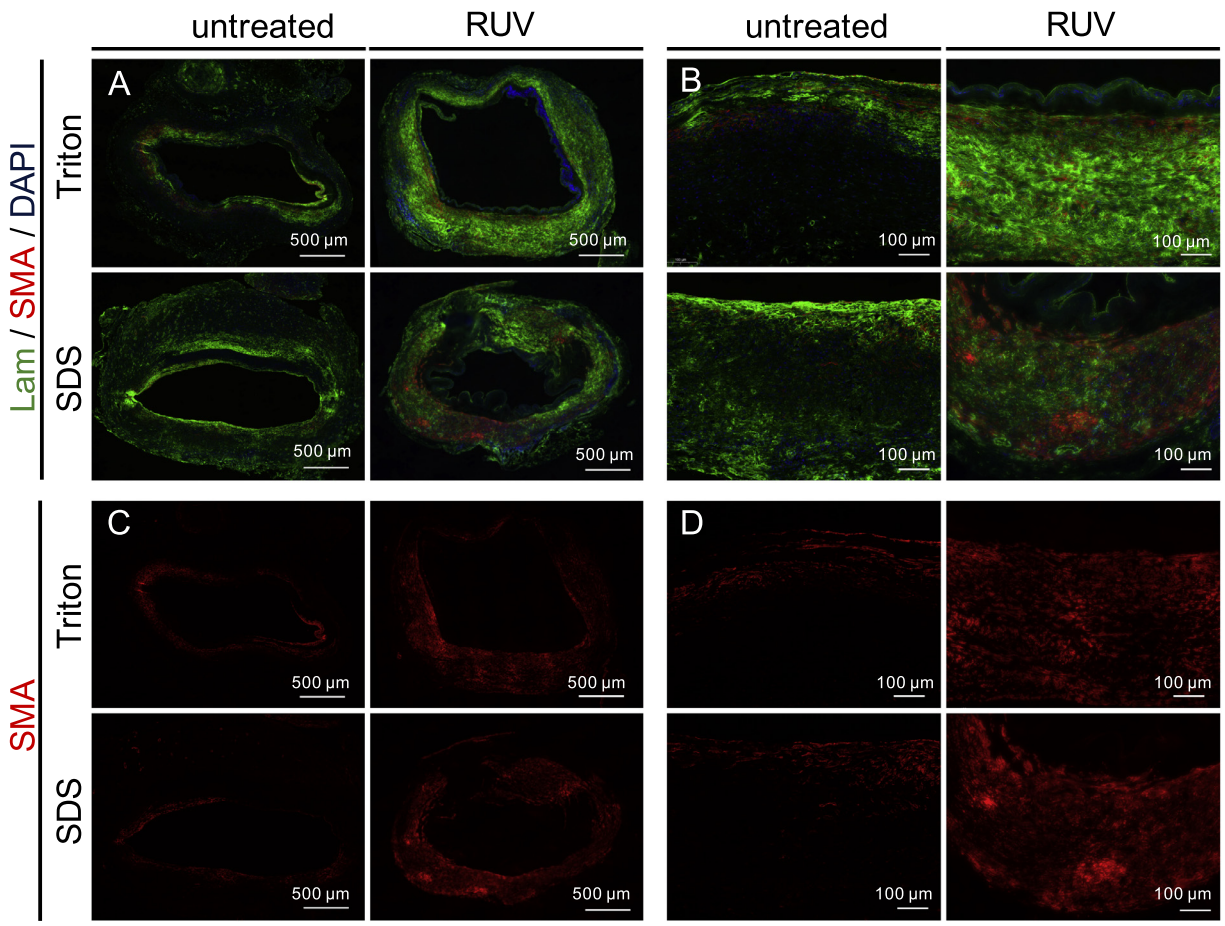

Fig. 6. Immunofluorescence staining of midgraft cross sections shows a deposition of laminin (Lam) and smooth muscle actin (SMA) one month after implantation. (A, B) merged channels (Lam/SMA/DAPI). (C, D) SMA channel only. All grafts show Lam and SMA positive stained areas. RUV treated grafts reveal SMA depositions in the whole graft walls, while SMA signals in untreated grafts were limited to the luminal area of the graft wall.

tics as a rough surface, or the absence of a functional endothelium may cause thrombotic events after implantation [39] and inappropriate degradation rates may influence the possibility of calcification [40] or aneurysm formation, which severely limits the long-term performance of vascular grafts [41].

In the present study, we investigated the use of riboflavin-mediated UV (RUV) crosslinking to improve the characteristics of decellularized small diameter vascular grafts derived from placental chorionic arteries. Riboflavin has been shown to increase UV absorption in collagenous tissue and therefore facilitates UV-induced collagen cross-linking. Noteably, if this effect is due to the creation of reactive oxygen species or photodynamic-processes is not completely understood [42].

The results of this study suggest that the RUV treatment improves surface smoothness and ultimate mechanical strength without detrimental effects on graft elasticity. Compared to untreated controls cell migration and tissue remodeling were not impaired, as it was often observed when using chemical crosslinking strategies [43].

Previously, we have shown that Triton-X100 or SDS decellularization successfully remove cells and their components from small arteries isolated from the human placenta chorionic plate. However, ultrastructural changes of the decellularized matrix graft were evident and were associated with disruptive properties of detergents [14]. Besides decreased biomechanical strength of the matrix grafts, decellularization treatment leads to exposure of collagen fibers with only low amount of remnants of basement membrane on the luminal surface, which may induce platelet aggregation and thrombosis leading to immediate graft occlusion after implantation [44]. Therefore, we intended to further improve the hemocompatibility and biomechanical strength of the decellularized matrix grafts to ensure safe application. In 2013, Ramesh et al. described the use of allogenic decellularized saphenous veins, which were crosslinked by dye-mediated photooxidation [45]. They have reported a favorable increase in biomechanical strength, hemocompatibility and smoothening of the luminal surface of the homografts when compared to native veins. The blood vessels were derived from human cadavers which may cause ethical concerns, especially when the final product should be commercialized. By contrast, our approach described here using placental vessels represents a suitable alternative to the use of blood vessels from human cadavers.

Human placental tissue, often only considered as a clinical waste product, has remarkable potential for its use in tissue engineering and can be harvested in large quantities without hesitation if an ethical approval and the informed consent of the patients is available [46,47]. We believe that decellularized arteries from the fetal part of the placenta, including the umbilical cord, have great potential to complement existing blood vessel replacement strategies, including autologous or cadaver donation. RUV crosslinking of the collagen matrix is a suitable method to further improve graft characteristics.

In this study, RUV crosslinking proved to smoothen the luminal graft surface, and prevented the exposure of collagen fibers, which significantly reduced platelet adhesion compared to untreated controls *in vitro*. No cytotoxic effect was observed during treatment,

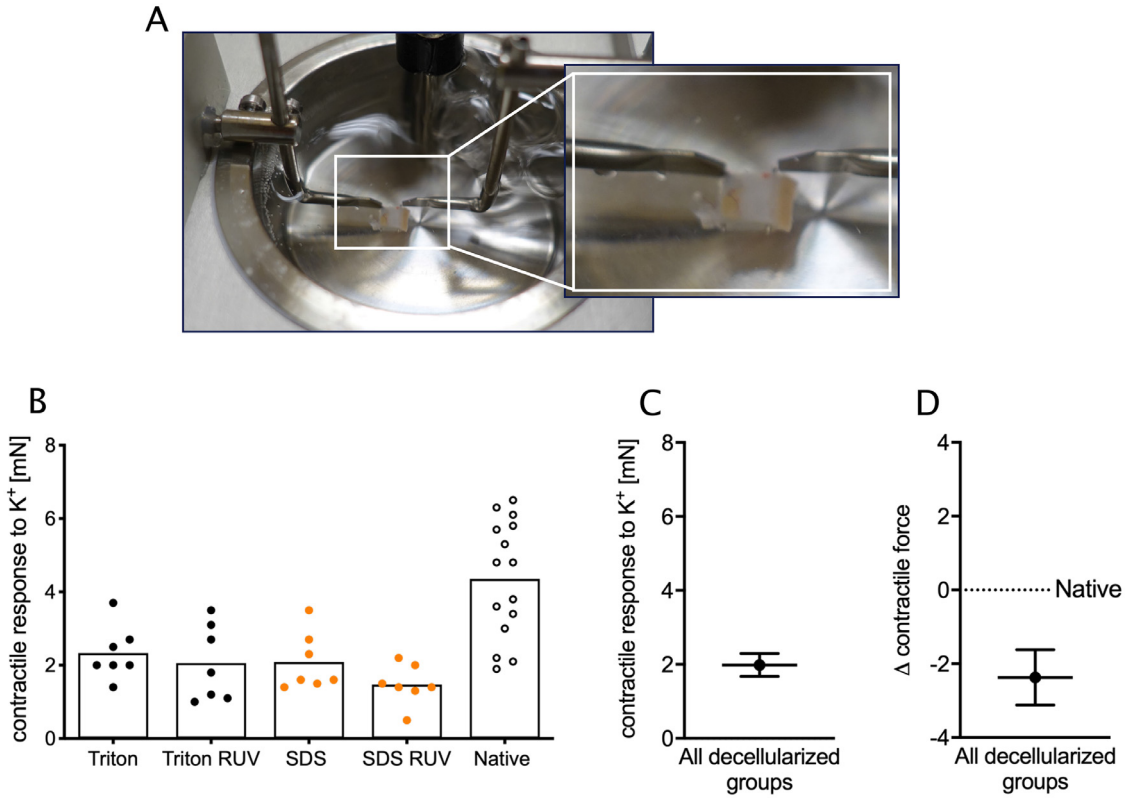

Fig. 7. Vasoconstrictive response of matrix grafts after stimulation with potassium in an organic bath of a DMT myograph system. (A) A 2 mm segment of a vascular graft mounted to the steel pins in the myograph chamber. (B) Raw data with mean values. (C) Confidence interval showing the estimated mean contraction force with its 95% confidence interval, which does not include 0, indicating that the contraction force was significantly higher than 0. (D) Estimated difference between all native and all other grafts with 95% confidence interval. Estimated mean contraction force values of decellularized grafts were significantly lower compared to contraction of native vessels.

and the graft surfaces showed high wettability, indicated by low contact angles between 33 and 40 degrees before and after RUV crosslinking. A hydrophilic graft surface indicates a high cell-matrix affinity [48,49], which correlates with our findings showing unimpeded cell growth of endothelial cells *in vitro* and the formation of a confluent endothelial layer *in vivo*.

An in vitro collagenase II (MMP-8) digestion assay of small diameter vascular grafts was performed to visualize the effects of graft modification steps (RUV and heparinization) on the degradation rate. MMP-8 was used because it is always the predominant collagenase in normal wound healing. This experiment revealed that only RUV-crosslinked samples showed a slight delay in degradation at early times (15 and 30 min). After 90 min, all samples were fully digested (Suppl. Fig. 3).

Biomechanical tests revealed significantly improved tensile strength of RUV treated grafts. Suture retention strength was significantly increased. In comparison, natural tissues like the saphenous vein and the internal mammary artery have suture retention strengths in the range of 90–140 g [50]. RUV crosslinking also significantly increased the burst pressure of the small diameter, thin-walled decellularized grafts by an average value of 900 mmHg to more than 2300 mmHg. According to the literature, physiological human saphenous veins exhibit an average burst pressure of 1260 ± 230 mmHg, while the internal mammary arteries reveals values between 1523 ± 654 mmHg and 3169 ± 1026 mmHg [51-54].

High patency rates of autologous grafts are not only due to their confluent endothelial layer. It is hypothesized that among other factors the compliance represents a main factor for graft patency [55]. As shown by Smith et al. adaption of vascular graft compliance at the anastomoses sites to the host vessel compliance at the anastomoses sites led to improved patency rates [56]. The anatomical structure of the grafts also plays an important role. The saphenous vein has been shown to be easily accessible to the surgeon, but elastic arteries like the internal mammary artery have proven to be even better vascular substitutes as they show optimal compliance and are not affected by atherosclerosis [57], leading to 90% patency after 7–10 years of implantation [58–60]. Furthermore, functional remodeling of vascular grafts is an important factor for successful long-term application.

In the present study it has to be emphasized, that RUV crosslinking did not affect graft compliance, although it caused a significant increase in biomechanical strength and burst pressure of the fabricated implants. However, there was a distinct decrease of graft compliance evident after short-term implantation (30 days), possibly due to rapid cell migration and vascular graft remodeling. It can be speculated that the high systemic blood pressure in the aorta of the rat induced rapid remodeling of the originally thin graft wall (200–400 µm). Species differences may be further relevant because we implanted human placental grafts into a rodent model. However, histology and blood profiles did not indicate severe immunogenic reactions (Suppl. Fig. 6 & 7). The resulting compliance after *in vivo* application of the grafts was still higher than in most tissue engineered grafts prior implantation [61,62]. Nevertheless, further observations are needed to evaluate the remodeling process during long-term application in a large animal model.

Prior to implantation, all grafts used in this study were heparinized by EDC coupling as described before [63], whereby a systematic anticoagulation was not necessary during and after

the surgical intervention. After 30 days, histological examination showed complete reendothelialization of the luminal surface of all grafts, and no signs of thrombus formation indicating that the anticoagulative effect of heparinization appears to be active until the reendothelialized surface is able to provide sufficient thromboresistance via biochemical processes regulating intrinsic and extrinsic coagulation pathways [64].

During the 1 month of implantation grafts showed appropriate performance and no failure modes. There were no signs of lumen narrowing, vasodilatation or aneurysm formation. No severe systemic or local inflammation was observed in the animals even though the xenogenic setup. Only low numbers of inflammatory cells (CD3, CD20, CD68 positive cells) were found in the graft wall. There was no indication of undesired calcified areas. Both, untreated and RUV crosslinked grafts enabled cell migration into the vessel wall and functional remodeling also indicated by functional stimulation tests. The repopulation of the grafts was not affected by the different decellularization methods nor by the RUV treatment and grafts revealed a dense population of differentiated desmin- and calponin-positive muscle cells only after one month of implantation. Several studies showed a strong effect of laminin on endothelial cell attachment and proliferation [65]. We observed the expression of laminin in the luminal area in untreated and RUV treated grafts after 1-month of implantation. However, RUV treated samples showed a distribution of laminin as well as smooth muscle actin predominantly in the medial and adventitial area of the graft wall. We speculate that RUV activates mechanisms of graft healing and aortic vessel wall maturation. It was shown in rats, that there is a constant increase in aortic laminin and actin expression between week 5 and 12 during development [66]. This expression is important for the maturation of the smooth muscle cell phenotype. Furthermore, it has been demonstrated that the ingrowth and proliferation of smooth muscle cells into the graft wall of synthetic, as well as autologous vein grafts is an indicator for graft healing [67–69]. Both, untreated and RUV crosslinked grafts enabled cell migration into the vessel wall and functional remodeling. The repopulation of the grafts was not affected by the different decellularization methods nor by the RUV treatment and grafts revealed a dense population of migrated cells after one month of implantation. Smooth muscle function was confirmed by contractile response to potassium stimulation in all grafts indicating the restoration of a functional muscular layer.

5. Conclusion

The design of a successful vascular graft with all the desirable characteristics like a non-thrombogenic surface, sufficient mechanical strength, resistance to intimal hyperplasia and compatibility with the host tissue remains challenging. Decellularized matrix grafts seem to be promising candidates to overcome these limitations especially when additional matrix modifications are used to compensate destructive changes during fabrication. In this study we demonstrate that RUV crosslinking is an effective approach to improve the characteristics of decellularized matrix grafts ensuring adequate biomechanical properties and host cell infiltration promoting subsequent graft remodeling.

6. Limitations of the study

The limitations of the study refer to the use of a small animal model, as rats show differences in comparative physiology (thrombogenicity, hemodynamics). However, the rat model is widely accepted for early-proof of concept studies to assess the biocompatibility and function of the graft before large animal experiments are performed. Further investigations are necessary to validate the convincing results of this research in a large animal, long-term implantation model using grafts with clinically relevant specifications.

Declaration of Competing Interest

The authors have no conflict of interest to declare.

CRediT authorship contribution statement

Karl H. Schneider: Conceptualization, Data curation, Formal analysis, Writing - original draft. **Sabrina Rohringer:** Data curation, Formal analysis. **Barbara Kapeller:** Data curation, Formal analysis. **Christian Grasl:** Data curation. **Herbert Kiss:** Data curation, Writing - review & editing. **Stefan Heber:** Formal analysis, Writing - review & editing. **Ingrid Walter:** Formal analysis. **Andreas H. Teuschl:** Data curation, Formal analysis, Writing - review & editing. **Bruno K. Podesser:** Formal analysis, Writing - review & editing, Funding acquisition. **Helga Bergmeister:** Conceptualization, Data curation, Formal analysis, Writing - original draft, Funding acquisition.

Acknowledgements

The authors want to thank Barbara Messner and her group, Medical University of Vienna, Surgical Research Laboratories-Cardiac Surgery, for providing access to the scanning electron microscope and Ricardo Vidal Da Silva from i3S - Instituto de Investigação e Inovação em Saúde, Universidade do Porto, for conducting the contact angle measurements and Claudia Höchsmann and Stefan Kummer from the VetCore Facility for Research, University of Veterinary Medicine Vienna for their expert technical assistance. We are also are grateful for the work of Andreas Pils performing pilot experiments for this study during his bachelor thesis at the Center for Biomedical Research and Nikolaus Herzog for his support in the graphic design. The authors thank Prof. Edward Leonard (Columbia University, New York) for helpful comments and editing assistance. This project was funded by the Ludwig Boltzmann Gesellschaft, Austria.

Supplementary materials

Supplementary material associated with this article can be found, in the online version, at doi:10.1016/j.actbio.2020.08.037.

References

[1] R.B. Rutherford, A.N. Sidawy, B.A. Perler, Rutherford's vascular surgery and endovascular therapy, Elsevier, Philadelphia, 2019.
[2] A.H. Huang, L.E. Niklason, Engineering of arteries in vitro, Cell.Mol .Life Sci. 71 (11) (2014) 2103–2118.
[3] L.E. Niklason, W. Abbott, J. Gao, B. Klagges, K.K. Hirschi, K. Ulubayram, N. Conroy, R. Jones, A. Vasanawala, S. Sanzgiri, R. Langer, Morphologic and mechanical characteristics of engineered bovine arteries, J. Vasc. Surg. 33 (3) (2001) 628–638.
[4] L. Gui, L.E. Niklason, Vascular tissue engineering: building perfusable vasculature for implantation, Curr. Opin. Chem. Eng. 3 (2014) 68–74.
[5] H. Bergmeister, N. Seyidova, C. Schreiber, M. Strobl, C. Grasl, I. Walter, B. Messner, S. Baudis, S. Frohlich, M. Marchetti-Deschmann, M. Griesser, M. di Franco, M. Krssak, R. Liska, H. Schima, Biodegradable, thermoplastic polyurethane grafts for small diameter vascular replacements, Acta Biomater. 11 (2015) 104–113.
[6] S.L. Dahl, A.P. Kypson, J.H. Lawson, J.L. Blum, J.T. Strader, Y. Li, R.J. Manson, W.E. Tente, L. DiBernardo, M.T. Hensley, R. Carter, T.P. Williams, H.L. Prichard, M.S. Dey, K.G. Begelman, L.E. Niklason, Readily available tissue-engineered vascular grafts, Sci. Transl. Med. 3 (68) (2011) 68–69.
[7] R.B. Chard, D.C. Johnson, G.R. Nunn, T.B. Cartmill, Aorta-coronary bypass grafting with polytetrafluoroethylene conduits. Early and late outcome in eight patients, J. Thorac. Cardiovasc. Surg. 94 (1) (1987) 132–134.
[8] F.W. Hehrlein, M. Schlepper, F. Loskot, H.H. Scheld, P. Walter, J. Mulch, The use of expanded polytetrafluoroethylene (PTFE) grafts for myocardial revascularization, J. Cardiovasc. Surg. (Torino) 25 (6) (1984) 549–553.

[9] H. Bergmeister, R. Plasenzotti, I. Walter, C. Plass, F. Bastian, E. Rieder, W. Sipos, A. Kaider, U. Losert, G. Weigel, Decellularized, xenogeneic small-diameter arteries: transition from a muscular to an elastic phenotype in vivo, J. Biomed. Mater. Res. B Appl. Biomater. 87 (1) (2008) 95–104.

[10] U. Boer, A. Lohrenz, M. Klingenberg, A. Pich, A. Haverich, M. Wilhelmi, The effect of detergent-based decellularization procedures on cellular proteins and immunogenicity in equine carotid artery grafts, Biomaterials 32 (36) (2011) 9730–9737.

[11] L. Mancuso, A. Gualerzi, F. Boschetti, F. Loy, G. Cao, Decellularized ovine arteries as small-diameter vascular grafts, Biomed. Mater. 9 (4) (2014) 045011.

[12] C.E. Schmidt, J.M. Baier, Acellular vascular tissues: natural biomaterials for tissue repair and tissue engineering, Biomaterials 21 (22) (2000) 2215–2231.

[13] A.F. Pellegata, M.A. Asnaghi, I. Stefani, A. Maestroni, S. Maestroni, T. Dominioni, S. Zonta, G. Zerbini, S. Mantero, Detergent-enzymatic decellularization of swine blood vessels: insight on mechanical properties for vascular tissue engineering, Biomed. Res. Int. 2013 (2013) 918753.

[14] K.H. Schneider, M. Enayati, C. Grasl, I. Walter, L. Budinsky, G. Zebic, C. Kaun, A. Wagner, K. Kratochwill, H. Redl, A.H. Teuschl, B.K. Podesser, H. Bergmeister, Acellular vascular matrix grafts from human placenta chorion: Impact of ECM preservation on graft characteristics, protein composition and in vivo performance, Biomaterials 177 (2018) 14–26.

[15] S.F. Badylak, D. Taylor, K. Uygun, Whole-organ tissue engineering: decellularization and recellularization of three-dimensional matrix scaffolds, Annu. Rev. Biomed. Eng. 13 (2011) 27–53.

[16] D.M. Faulk, C.A. Carruthers, H.J. Warner, C.R. Kramer, J.E. Reing, L. Zhang, A. D'Amore, S.F. Badylak, The effect of detergents on the basement membrane complex of a biologic scaffold material, Acta Biomater. 10 (1) (2014) 183–193.

[17] J.C. Fitzpatrick, P.M. Clark, F.M. Capaldi, Effect of decellularization protocol on the mechanical behavior of porcine descending aorta, Int. J. Biomater. 2010 (2010).

[18] K.H. Schneider, P. Aigner, W. Holnthoner, X. Monforte, S. Nurnberger, D. Runzler, H. Redl, A.H. Teuschl, Decellularized human placenta chorion matrix as a favorable source of small-diameter vascular grafts, Acta Biomater. 29 (2016) 125–134.

[19] C. Williams, J. Liao, E.M. Joyce, B. Wang, J.B. Leach, M.S. Sacks, J.Y. Wong, Altered structural and mechanical properties in decellularized rabbit carotid arteries, Acta Biomater. 5 (4) (2009) 993–1005.

[20] Y. Zou, Y. Zhang, Mechanical evaluation of decellularized porcine thoracic aorta, J. Surg. Res. 175 (2) (2012) 359–368.

[21] S. Guler, B. Aslan, P. Hosseinian, H.M. Aydin, Supercritical Carbon Dioxide-Assisted Decellularization of Aorta and Cornea, Tissue Eng. Part C Methods 23 (9) (2017) 540–547.

[22] Q. Xing, K. Yates, M. Tahtinen, E. Shearier, Z. Qian, F. Zhao, Decellularization of fibroblast cell sheets for natural extracellular matrix scaffold preparation, Tissue Eng. Part C Methods 21 (1) (2015) 77–87.

[23] P.M. Crapo, T.W. Gilbert, S.F. Badylak, An overview of tissue and whole organ decellularization processes, Biomaterials 32 (12) (2011) 3233–3243.

[24] K.H. Hussein, K.M. Park, K.S. Kang, H.M. Woo, Biocompatibility evaluation of tissue-engineered decellularized scaffolds for biomedical application, Mater. Sci. Eng. C Mater. Biol. Appl. 67 (2016) 766–778.

[25] K.H. Schneider, P. Aigner, W. Holnthoner, X. Monforte, S. Nurnberger, D. Runzler, H. Redl, A.H. Teuschl, Decellularized human placenta chorion matrix as a favorable source of small-diameter vascular grafts, Acta Biomater. 29 (2016) 125–134.

[26] R. Parenteau-Bareil, R. Gauvin, F. Berthod, Collagen-based biomaterials for tissue engineering applications, Materials 3 (3) (2010) 1863–1887.

[27] J.W. Drexler, H.M. Powell, Dehydrothermal crosslinking of electrospun collagen, Tissue Eng. Part C Methods 17 (1) (2011) 9–17.

[28] M. Hara, Various cross-linking methods for collagens: merit and demerit of methods by radiation, J. Oral Tissue Eng. 3 (3) (2006) 118–124.

[29] H. Rich, M. Odlyha, U. Cheema, V. Mudera, L. Bozec, Effects of photochemical riboflavin-mediated crosslinks on the physical properties of collagen constructs and fibrils, J. Mater. Sci. Mater. Med. 25 (1) (2014) 11–21.

[30] M.A. Moore, A.K. Adams, Calcification resistance, biostability, and low immunogenic potential of porcine heart valves modified by dye-mediated photooxidation, J. Biomed. Mater. Res. 56 (1) (2001) 24–30.

[31] B. Meuris, R. Phillips, M.A. Moore, W. Flameng, Porcine stentless bioprostheses: prevention of aortic wall calcification by dye-mediated photo-oxidation, Artif Organs 27 (6) (2003) 537–543.

[32] R.J. Lomas, J.E. Cruse-Sawyer, C. Simpson, E. Ingham, R. Bojar, J.N. Kearney, Assessment of the biological properties of human split skin allografts disinfected with peracetic acid and preserved in glycerol, Burns 29 (6) (2003) 515–525.

[33] H. Bergmeister, C. Schreiber, C. Grasl, I. Walter, R. Plasenzotti, M. Stoiber, D. Bernhard, H. Schima, Healing characteristics of electrospun polyurethane grafts with various porosities, Acta Biomater. 9 (4) (2013) 6032–6040.

[34] ISO, Cardiovascular implants- Tubular vascular prostheses, ISO 7198:2016, 1998.

[35] R. Dhurat, M. Sukesh, Principles and Methods of Preparation of Platelet-Rich Plasma: A Review and Author's Perspective, J. Cutan. Aesthet Surg. 7 (4) (2014) 189–197.

[36] B. Romeis, M. Mulisch, U. Welsch, Romeis Mikroskopische Technik (2010).

[37] J. Schindelin, I. Arganda-Carreras, E. Frise, V. Kaynig, M. Longair, T. Pietzsch, S. Preibisch, C. Rueden, S. Saalfeld, B. Schmid, J.Y. Tinevez, D.J. White, V. Hartenstein, K. Eliceiri, P. Tomancak, A. Cardona, Fiji: an open-source platform for biological-image analysis, Nat Methods 9 (7) (2012) 676–682.

[38] Y. Ma, X.Y. Cao, X.J. Feng, Y.M. Ma, H. Zou, Fabrication of super-hydrophobic film from PMMA with intrinsic water contact angle below 90 degrees, Polymer 48 (26) (2007) 7455–7460.

[39] W.E. Burkel, D.W. Vinter, J.W. Ford, R.H. Kahn, L.M. Graham, J.C. Stanley, Sequential studies of healing in endothelial seeded vascular prostheses: histologic and ultrastructure characteristics of graft incorporation, J. Surg. Res. 30 (4) (1981) 305–324.

[40] T. Sugiura, S. Tara, H. Nakayama, T. Yi, Y.U. Lee, T. Shoji, C.K. Breuer, T. Shinoka, Fast-degrading bioresorbable arterial vascular graft with high cellular infiltration inhibits calcification of the graft, J. Vasc. Surg. 66 (1) (2017) 243–250.

[41] G.M. FitzGibbon, A.J. Leach, H.P. Kafka, W.J. Keon, Coronary bypass graft fate: long-term angiographic study, J. Am. Coll. Cardiol. 17 (5) (1991) 1075–1080.

[42] E. Letko, P.A. Majmudar, S.L. Forstot, R.J. Epstein, R.S. Rubinfeld, UVA-light and riboflavin-mediated corneal collagen cross-linking, Int. Ophthalmol. Clin. 51 (2) (2011) 63–76.

[43] J.D. Berglund, M.M. Mohseni, R.M. Nerem, A. Sambanis, A biological hybrid model for collagen-based tissue engineered vascular constructs, Biomaterials 24 (7) (2003) 1241–1254.

[44] M.J. Barnes, Collagen polymorphism in relation to the role of collagen-induced platelet aggregation in haemostasis and thrombosis, Prog. Clin. Biol. Res. 54 (1981) 163–182.

[45] B. Ramesh, S. Mathapati, S. Galla, K.M. Cherian, S. Guhathakurta, Crosslinked acellular saphenous vein for small-diameter vascular graft, Asian. Cardiovasc. Thorac. Ann. 21 (3) (2013) 293–302.

[46] K. Benirschke, Remarkable placenta, Clin. Anat. 11 (3) (1998) 194–205.

[47] A.R. Silini, A. Cargnoni, M. Magatti, S. Pianta, O. Parolini, The Long Path of Human Placenta, and Its Derivatives, in Regenerative Medicine, Front. Bioeng. Biotechnol. 3 (2015) 162.

[48] H. Zhu, J. Ji, J. Shen, Construction of multilayer coating onto poly-(DL-lactide) to promote cytocompatibility, Biomaterials 25 (1) (2004) 109–117.

[49] Y. Zhu, C. Gao, T. He, J. Shen, Endothelium regeneration on luminal surface of polyurethane vascular scaffold modified with diamine and covalently grafted with gelatin, Biomaterials 25 (3) (2004) 423–430.

[50] G. Konig, T.N. McAllister, N. Dusserre, S.A. Garrido, C. Iyican, A. Marini, A. Fiorillo, H. Avila, W. Wystrychowski, K. Zagalski, M. Maruszewski, A.L. Jones, L. Cierpka, L.M. de la Fuente, N. L'Heureux, Mechanical properties of completely autologous human tissue engineered blood vessels compared to human saphenous vein and mammary artery, Biomaterials 30 (8) (2009) 1542–1550.

[51] N. L'Heureux, N. Dusserre, G. Konig, B. Victor, P. Keire, T.N. Wight, N.A. Chronos, A.E. Kyles, C.R. Gregory, G. Hoyt, R.C. Robbins, T.N. McAllister, Human tissue-engineered blood vessels for adult arterial revascularization, Nat Med 12 (3) (2006) 361–365.

[52] N. L'Heureux, S. Paquet, R. Labbe, L. Germain, F.A. Auger, A completely biological tissue-engineered human blood vessel, FASEB J. 12 (1) (1998) 47–56.

[53] C.J. van Andel, P.V. Pistecky, C. Borst, Mechanical properties of porcine and human arteries: implications for coronary anastomotic connectors, Ann. Thorac. Surg. 76 (1) (2003) 58–64 discussion 64-5.

[54] M. Neufurth, X. Wang, E. Tolba, B. Dorweiler, H.C. Schroder, T. Link, B. Diehl–Seifert, W.E. Muller, Modular small diameter vascular grafts with bioactive functionalities, PLoS One 10 (7) (2015) e0133632.

[55] W.M. Abbott, J. Megerman, J.E. Hasson, G. L'Italien, D.F. Warnock, Effect of compliance mismatch on vascular graft patency, J. Vasc. Surg. 5 (2) (1987) 376–382.

[56] A. Tiwari, K.S. Cheng, H. Salacinski, G. Hamilton, A.M. Seifalian, Improving the patency of vascular bypass grafts: the role of suture materials and surgical techniques on reducing anastomotic compliance mismatch, Eur. J. Vasc. Endovasc. Surg. 25 (4) (2003) 287–295.

[57] F. Otsuka, K. Yahagi, K. Sakakura, R. Virmani, Why is the mammary artery so special and what protects it from atherosclerosis? Ann. Cardiothorac. Surg. 2 (4) (2013) 519–526.

[58] H.B. Barner, M.T. Swartz, J.G. Mudd, D.H. Tyras, Late patency of the internal mammary artery as a coronary bypass conduit, Ann. Thorac. Surg. 34 (4) (1982) 408–412.

[59] A.J. Tector, T.M. Schmahl, B. Janson, J.R. Kallies, G. Johnson, The internal mammary artery graft. Its longevity after coronary bypass, JAMA 246 (19) (1981) 2181–2183.

[60] C.M. Grondin, L. Campeau, J. Lesperance, M. Enjalbert, M.G. Bourassa, Comparison of late changes in internal mammary artery and saphenous vein grafts in two consecutive series of patients 10 years after operation, Circulation 70 (3 Pt 2) (1984) I208–I212.

[61] T. Fukunishi, C.A. Best, T. Sugiura, J. Opfermann, C.S. Ong, T. Shinoka, C.K. Breuer, A. Krieger, J. Johnson, N. Hibino, Preclinical study of patient-specific cell-free nanofiber tissue-engineered vascular grafts using 3-dimensional printing in a sheep model, J. Thorac. Cardiovasc. Surg. 153 (4) (2017) 924–932.

[62] J. O.D. Johnson, T. Groehl, S. Hetterscheidt, M. Jones, Development of Novel, Bioresorbable, Small-Diameter Electrospun Vascular Grafts, Tissue Sci. Eng. 6 (2015).

[63] B.S. Conklin, E.R. Richter, K.L. Kreutziger, D.S. Zhong, C. Chen, Development and evaluation of a novel decellularized vascular xenograft, Med. Eng. Phys. 24 (3) (2002) 173–183.

[64] J.W. Yau, H. Teoh, S. Verma, Endothelial cell control of thrombosis, BMC Cardiovasc. Disord. 15 (2015) 130.

[65] R. Hallmann, N. Horn, M. Selg, O. Wendler, F. Pausch, L.M. Sorokin, Expression and function of laminins in the embryonic and mature vasculature, Physiol. Rev. 85 (3) (2005) 979–1000.

[66] O. Kocher, O. Skalli, D. Cerutti, F. Gabbiani, G. Gabbiani, Cytoskeletal features of rat aortic cells during development. An electron microscopic, immunohistochemical, and biochemical study, Circ. Res. 56 (6) (1985) 829–838.
[67] J.E. O'Brien Jr., Y. Shi, A. Fard, T. Bauer, A. Zalewski, J.D. Mannion, Wound healing around and within saphenous vein bypass grafts, J. Thorac. Cardiovasc. Surg. 114 (1) (1997) 38–45.
[68] S.M. Scott, M.G. Barth, L.R. Gaddy, E.T. Ahl Jr., The role of circulating cells in the healing of vascular prostheses, J. Vasc. Surg. 19 (4) (1994) 585–593.
[69] T. Ueberrueck, L. Meyer, R. Zippel, G. Nestler, T. Wahlers, I. Gastinger, Healing characteristics of a new silver-coated, gelatine impregnated vascular prosthesis in the porcine model, Zentralbl. Chir. 130 (1) (2005) 71–76.